JOURNAL OF MATERIALS SCIENCE 31 (1996) 2631–2639

# Effects of $Y_2O_3$ and $La_2O_3$ addition on the crystallization of $Li_2O \cdot Al_2O_3 \cdot 4SiO_2$ glass–ceramic

JIIN-JYH SHYU, CHI-SHENG HWANG
*Department of Materials Engineering, Tatung Institute of Technology, Taipei, Taiwan*

Effects of adding $Y_2O_3$ and $La_2O_3$ on the crystallization of β-quartz solid solution (ss) and the subsequent β-quartz ss to β-spodumene transformation of $Li_2O \cdot Al_2O_3 \cdot 4SiO_2$ glass–ceramic were investigated. Adding $\geq 4$ mol% $YO_{3/2}$ or 8 mol% $LaO_{3/2}$ effectively improved the control of the crystallization process of the glass. $Y_2O_3$ did not effectively induce bulk crystallization of β-quartz ss, but can reduce the rate of surface crystallization. $La_2O_3$ completely suppressed the surface crystallization and promoted a uniform, bulk crystallization of β-quartz ss. For both the $Y_2O_3$- and $La_2O_3$-doped glasses, the kinetics for glass crystallization to β-quartz ss was delayed as the doping level increased. Except for the 8 mol% $LaO_{3/2}$-doped glass in which no β-spodumene was formed, the kinetics for the β-quartz ss to β-spodumene transformation for the doped glasses was enhanced compared with that for the undoped glass. For the 4 and 8 mol% $YO_{3/2}$-doped compositions, the relative amount of β-spodumene to β-quartz revealed an anomalous decrease trend with heating temperature in a particular temperature range. This can be explained by the surface crystallization characteristic, which induced an overlap of crystallization and β-quartz ss to β-spodumene transformation. Glass doped with 8 mol% $LaO_{3/2}$ exhibited an Avrami exponent of about 2.4 and an activation energy for crystal growth of β-quartz ss of about 418 kJ $mol^{-1}$.

## 1. Introduction

Glass–ceramics in the system $Li_2O$–$Al_2O_3$–$SiO_2$ (LAS), which contain β-spodumene (β-S, $Li_2O \cdot Al_2O_3 \cdot 4SiO_2$) and/or β-quartz solid solution (β-quartz ss, β-Q), are important for cooktop panels, stove windows, cookware, and some precision parts [1]. They have a very low and even negative coefficient of thermal expansion [2]. β-spodumene-containing glass–ceramics also have the potential to meet the dielectric constant and thermal expansion requirements for integrated circuit substrates [3–5]. It has been shown that the first crystalline phase formed in $Li_2O \cdot Al_2O_3 \cdot 4SiO_2$ ($LAS_4$) glass is β-Q, which then transforms into the stable β-S phase [2]. Careful control of β-S to β-Q ratio is important, because of the sizable difference in the coefficient of thermal expansion between β-Q formed from $LAS_4$ glass (about $-1.1 \times 10^{-6}\,K^{-1}$, 20–300°C [2]) and β-S ($0.9 \times 10^{-6}K^{-1}$, 200–1000°C [6]).

Controlled crystallization is a basic condition for the preparation of glass–ceramic materials. For the undoped, stoichiometric $LAS_4$ glass, uncontrolled surface crystallization is often observed, which would result in cracking of the products. Therefore, small additives such as $TiO_2$ and $ZrO_2$ are often used in the LAS system to improve the above nature [6]. However, little work has been conducted to evaluate the effect of other additives. In this paper, the effects of $Y_2O_3$ and $La_2O_3$ as dopants on the crystallization and the subsequent β-Q to β-S transformation in the $LAS_4$ glass–ceramic were examined.

## 2. Experimental procedure

### 2.1. Sample preparation

The nominal compositions of the glasses studied are listed in Table I. The $Li_2O$:$Al_2O_3$:$SiO_2$ ratio is 1:1:4 for all glasses. Glass N is the stoichiometric spodumene ($Li_2O \cdot Al_2O_3 \cdot 4SiO_2$). All raw materials used to prepare the glasses were reagent grade. Each glass was melted at 1650°C for 10 h in a platinum crucible and then quenched by pouring it onto a copper plate. The glasses were annealed at 600°C for 2 h and then furnace-cooled to room temperature. The

TABLE I Nominal mol% compositions of glasses studied

| Glass | $Li_2O$ | $Al_2O_3$ | $SiO_2$ | $YO_{3/2}$ | $LaO_{3/2}$ |
|---|---|---|---|---|---|
| N | 16.63 | 16.63 | 66.52 | | |
| Y0 | 16.12 | 16.69 | 66.76 | 0.43 | |
| Y4 | 16.00 | 16.00 | 64.00 | 4 | |
| Y8 | 15.97 | 15.97 | 63.89 | 8.33 | |
| L0 | 16.60 | 16.60 | 66.38 | | 0.43 |
| L4 | 16.00 | 16.00 | 64.00 | | 4 |
| L8 | 15.33 | 15.33 | 61.33 | | 8 |

0022–2461 

as-annealed glasses were cut by diamond saw to yield cubes ($6 \times 6 \times 6\ mm^3$). Samples were heated at typically 800–1200 °C for 1 h to convert the glasses into glass–ceramics. The heating rate was 10 K $min^{-1}$.

## 2.2. Characterization

Glass samples were crushed into powders (60–80 mesh) for the differential thermal analysis (DTA) measurements. The precipitated crystalline phases were identified by X-ray diffraction (XRD) analysis using powder or bulk samples. Measurements were performed on a diffractometer operating at 40 kV and 15 mA. Continuous scanning was used with a scan speed of 2° $min^{-1}$ and a sampling interval of 0.05° (2θ). The crystallized samples were polished, etched with 1 wt% HF for 30 s, and then coated with a thin film of gold for scanning electron microscopy (SEM) observations.

# 3. Results and discussion

## 3.1. Visual examination of the as-annealed and crystallized glasses

To some extent, surface-vitrification occurred during annealing of the glasses N, Y0, L0, and L4, resulting in various degrees of cracking. The vitrified parts of the as-annealed glasses were removed by diamond saw. After heating these glasses at the crystallizing temperatures, the cross-section revealed a layer about 1–2 mm thick growing from the sample surface as a result of surface crystallization, while the interior region was still amorphous. This observation indicates that for these glasses there was a strong tendency for uncontrolled surface crystallization while bulk crystallization was nearly absent.

In contrast, the as-annealed Y4, Y8, and L8 glasses were transparent, clear, and crack-free. No evidence of vitrification was observed. For the crystallized Y4 and Y8 samples, a surface layer as well as some small cracks which are oriented perpendicular to the sample surface developed. However, no fracturing occurred. For the crystallized L8 samples, no surface layer developed and uniform, bulk crystallization without cracking was observed. These results indicate that the crystallization of these glasses occurs in a controlled manner.

## 3.2. Effect of $Y_2O_3$

Fig. 1 shows the powder XRD patterns used to examine the crystallization of glass to β-Q (G → Q) for the $Y_2O_3$-doped glasses. Samples were heated for 1 h at temperatures ≤ 850 °C. For the heating temperature of 800 °C, sample N (curve a) showed a remarkable amount of β-Q. Adding 0.4% Y (curve b) substantially reduced the crystallization rate. Adding 4% and 8% Y (curves c and d, respectively) completely suppressed

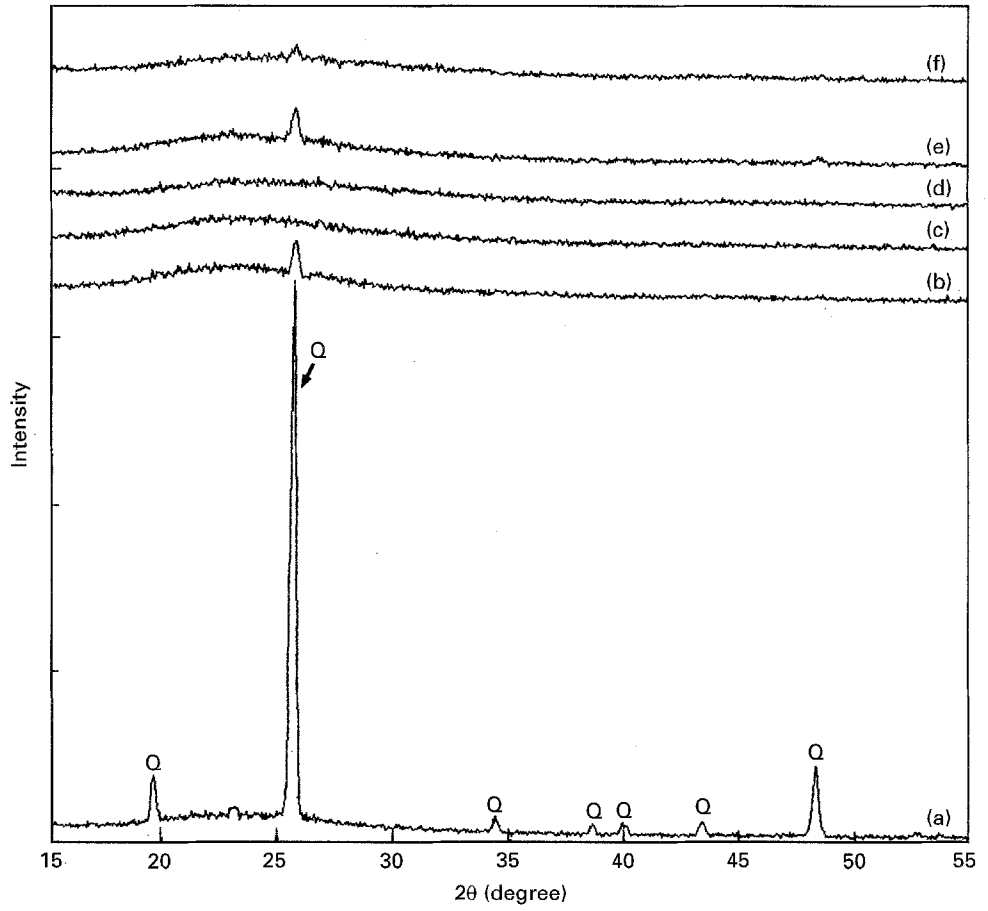


*Figure 1* Powder XRD patterns to examine the crystallization of glass to β-quartz ss for the $Y_2O_3$-doped glasses. (a) N, 800 °C/1 h, (b) Y0, 800 °C/1 h, (c) Y4, 800 °C/1 h, (d) Y8, 800 °C/1 h, (e) Y4, 850 °C/1 h, and (f) Y8, 850 °C/1 h. (Q: β-quartz ss).

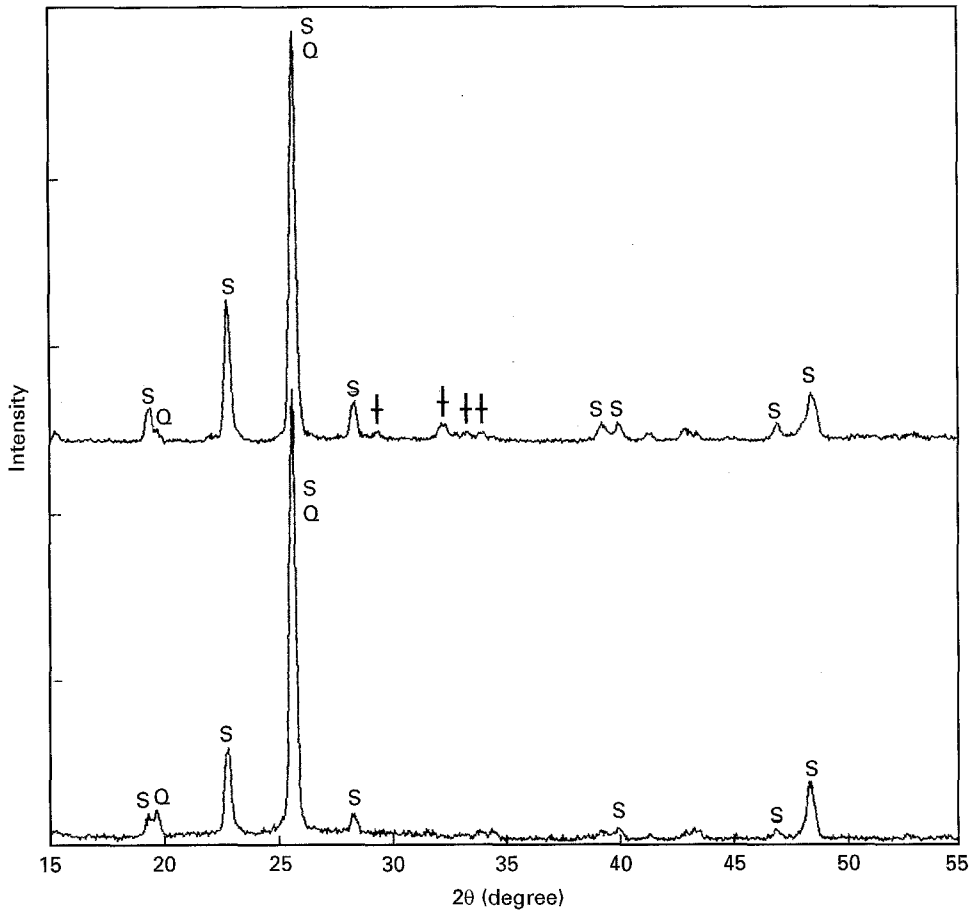


*Figure 2* Powder XRD patterns of the Y4 samples heated at (a) 900 °C and (b) 1000 °C for 1 h. (Q: β-quartz ss, S: β-spodumene, †: $Y_7S_9$).

crystallization. At 850 °C, Y4 (curve e) revealed a higher amount of β-Q than Y8 (curve f). According to these results and the observed surface-layer described in Section 3.1, it is concluded that although $Y_2O_3$ did not effectively induce bulk nucleation of β-Q, the rate of surface nucleation can be reduced. This conclusion explains the improvement in crystallization behaviour described in Section 3.1 for Y4 and Y8 compared with N and Y0.

Typical powder XRD patterns for the $Y_2O_3$-doped samples heated at higher temperatures are shown in Fig. 2. It can be seen that the transformation from β-Q to β-S (Q → S) occurred. Furthermore, samples Y4 and Y8 heated at temperatures ≥ 1000 °C give X-ray lines most likely corresponding to the $7Y_2O_3 \cdot 9SiO_2$ ($Y_7S_9$) phase. Fig. 3 shows the relative X-ray intensity of β-S to β-Q, $I_{s,111}/(I_{s,111} + I_{Q,100})$, as a function of heating temperature for all the $Y_2O_3$-doped glasses. It is well known that for the spodumene-containing glass–ceramics the first crystalline phase precipitated is β-Q, which then transforms into the stable β-S phase [2]. Since the glass cannot directly crystallize into β-S, a decrease in the G → Q kinetics may imply a decrease in the Q → S kinetics (or a higher onset temperature of Q → S transformation, $T_{Q\to S}$). It can be seen in Fig. 1 that all the $Y_2O_3$-doped glasses showed substantially delayed G → Q kinetics compared with glass N, while their $T_{Q\to S}$ (Fig. 3) are lower than that for N. This result suggests that in the present study the crystallization G → Q kinetics did not significantly

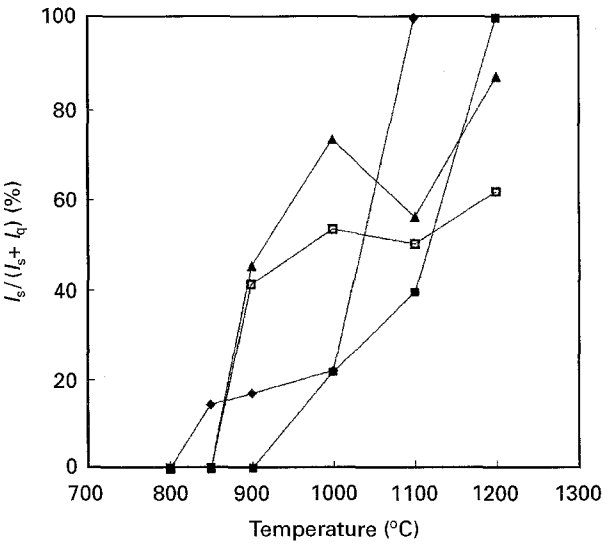


*Figure 3* The relative X-ray intensity of β-S to β-Q, $I_{s,111}/(I_{s,111} + I_{Q,100})$, as a function of heating temperature for the $Y_2O_3$-doped samples. Key: ■ N; ◆ Y0; ▲ Y4; □ Y8.

influence the kinetics of the subsequent Q → S transformation. Therefore, it is also suggested that $Y_2O_3$ reduces the stability of the β-Q crystal formed, thus reducing $T_{Q\to S}$ for the $Y_2O_3$-containing samples.

Furthermore, it can be seen in Fig. 3 that the relative β-S content for both N and Y0 increased continuously with increasing heating temperature. This

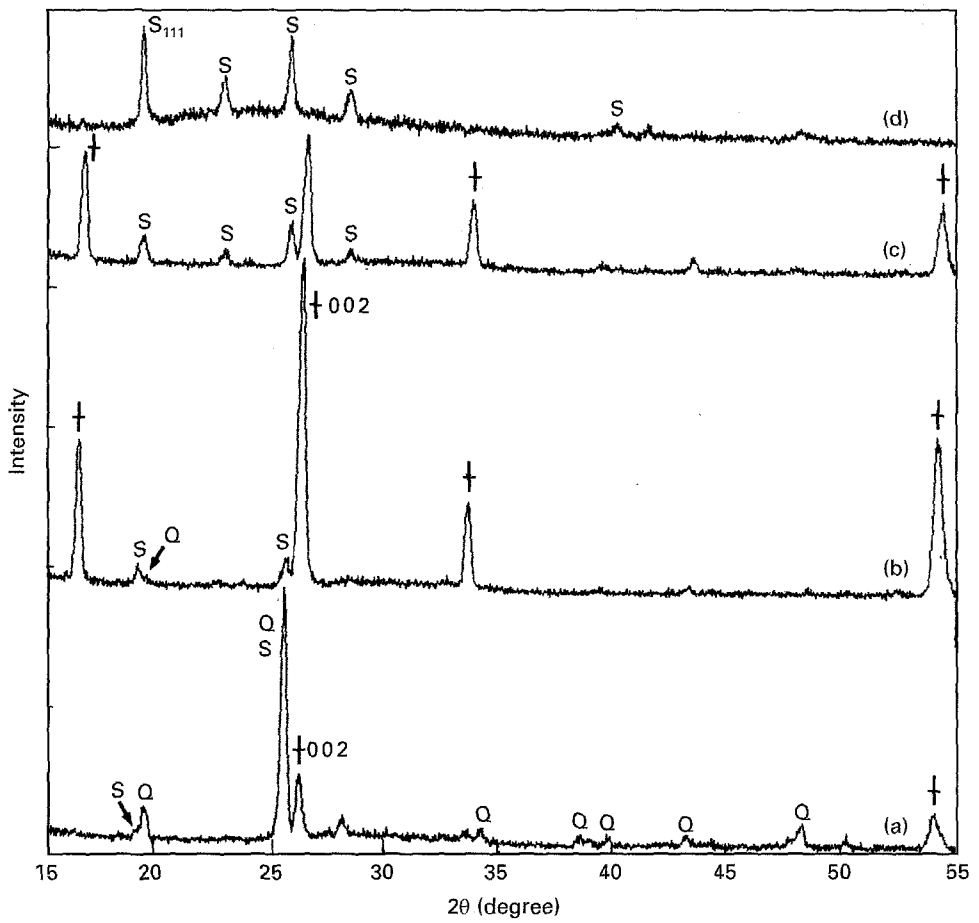


*Figure 4* XRD patterns of the L4 sample heated at 900 °C for 1 h. (a) free surface, (b) 0.5, (c) 1.5, and (d) 2.5 mm depth under the free surface. (Q: β-quartz ss, S: β-spodumene, †: $Y_7S_9$).

behaviour is usually observed in the literature for spodumene-containing glass–ceramics. Moreover, the relative β-S content increased as Y content was increased from 0 to 4%. However, Y4 and Y8 showed a different behaviour from that described above for N and Y0. First, the relative β-S amount for both Y4 and Y8 samples revealed an anomalous decreasing trend between 1000 and 1100 °C. Second, the relative β-S amount was lowered as Y content was increased from 4 to 8%.

To explore the above anomalous nature for Y4 and Y8 compositions, detailed information about the phase distribution from the surface to the bulk of the crystallized samples was examined by polishing the samples to the desired depth and analysing the crystal phases of the sample surface with XRD. Fig. 4 shows the typical XRD spectra for the Y4 sample heated at 900 °C for 1 h. All the spectra reveal that β-Q, β-S, and $Y_7S_9$ were the crystalline phases formed. As shown in pattern (a), the major crystalline phase on the free surface is β-Q. The peaks of β-S and $Y_7S_9$ are small. The preferred (0 0 *l*) orientation of $Y_7S_9$ indicates a surface-crystallization behaviour of this phase. After polishing the free surface to remove about 0.5 mm of material (pattern (b)), $Y_7S_9$ became the major crystalline phase. The β-S peaks are weak and the β-Q phase nearly vanished. For the depth of 1.5 mm (pattern (c)), the main crystalline phase is still $Y_7S_9$ but with a lower relative intensity than that for the 0.5 mm spectrum. The intensity for β-S phase increased and the peaks for β-Q have completely vanished. As the surface layer was removed completely (pattern (d)), the $Y_7S_9$ phase disappeared and β-S with a high level of residual glass phase was seen. Note that all the above patterns (a)–(d) reveal a (1 1 1) preferred orientation of β-S phase, indicating a surface-related crystallization

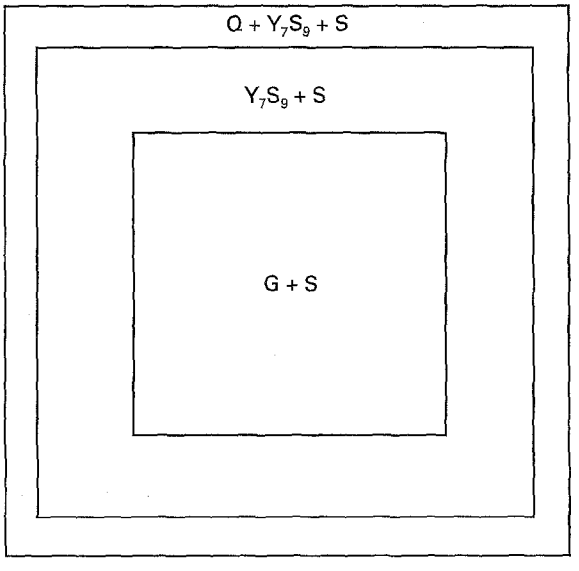


*Figure 5* Schematic drawing to show the phase distribution in the L4 sample heated at 900 °C for 1 h.

of this phase. Therefore, the β-S intensity for the bulk region (pattern (d)) was mainly caused by some of the β-S grains which grew from the surface layer and have faster growth rates than the average.

The results from Fig. 4 are shown schematically in Fig. 5 and are explained as follows. β-Q first crystallized from the sample surface (pattern (a)). The high nucleation density of β-Q on the sample surface was responsible for the small amount of $Y_7S_9$ in this region. Since most of the uncrystallized $Y_2O_3$ content was moved from the surface region toward the interior, a substantial amount of $Y_7S_9$ crystallized under the free surface (patterns (b) and (c)) and grew toward the interior region. According to the above patterns, as the bulk region was approached, the amount of β-Q suddenly decreased while that of β-S increased. This behaviour might be caused by a grain-size effect, i.e. small-grained β-Q is more resistant to transformation into β-S. Since the β-Q crystals formed in the free surface region were small, most of them were resistant to transforming into β-S, as shown in pattern (a). Some of the β-Q grains which exhibited faster growth rates (these grains should have some habit crystallographic direction perpendicular to the sample surface), can grow continuously toward the centre of the sample. These β-Q crystals can grow to large sizes due to the low crystal density in the interior region. As a result, they can transform into β-S phase with a (1 1 1) preferred orientation.

The decreasing trend of the relative amount of β-S in the temperature range of 1000–1100 °C for the Y4 and Y8 compositions, as seen in Fig. 3, can be explained according to Fig. 5. As the heating temperature was further increased, the residual glass region would crystallize into β-Q. Therefore, some extent of overlap of G → Q and Q → S transformations occurred. This overlap is more significant for compositions in which the G → Q transformation is shifted to a higher temperature and the instability of β-Q crystal is reduced to a lower temperature, as seen in Y4 and Y8. Thus, a decrease in the relative amount of β-S was observed in a particular temperature range.

Fig. 6a and b show typical microstructures for the $Y_2O_3$-doped samples. According to Fig. 6a, the elongated morphology with the highly oriented characteristic of the $Y_7S_9$ particles is evident,which is in agreement with the XRD result described in Fig. 4. Fig. 6b shows the microstructure in the bulk region. The degree of preferred orientation of the $Y_7S_9$ phase decreased. Moreover, the β-S particles are distributed in the matrix.

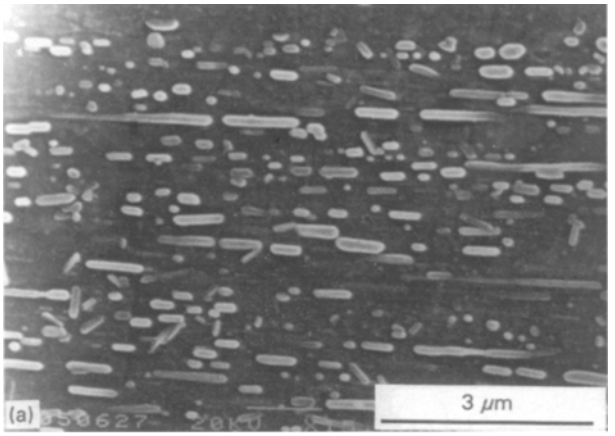


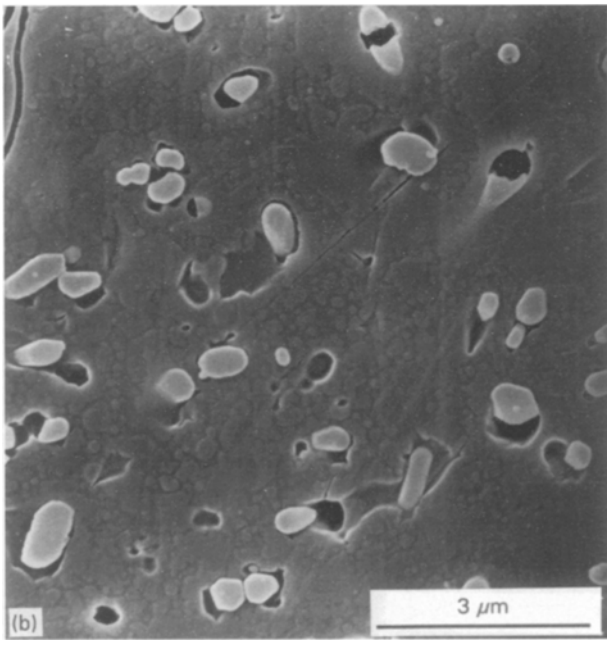


*Figure 6* SEM pictures showing the microstructures of the Y4 sample heated at 1200 °C for 1 h. (a) surface region and (b) bulk region. (Bar = 3 μm).

## 3.3. Effect of $La_2O_3$

Fig. 7 shows the powder XRD patterns of the La-series samples heated for 1 h at 800 °C. All samples revealed only β-Q phase. The crystallizability of the β-Q phase was not influenced by the addition of 0.4% La (curves (a) and (b)), while it was considerably suppressed as the La content was increased to 4%. Since no bulk crystallization was induced, as described in Section 3.1, for glass L4, this decreased crystallizability is attributed to the reduced rate of surface crystallization. The L8 sample showed an increased amount of β-Q compared with the L4 sample. This result can be explained by the enhanced bulk crystallization, as described in Section 3.1. Actually, for L8 samples heated at 800–1200 °C, no surface layer can be seen under SEM examination, indicating that the surface crystallization was completely suppressed.

Heating the L0 and L4 glasses at higher temperatures resulted in Q → S phase transformation. For L8 samples heated at 800–1200 °C, however, the Q → S transformation was nearly suppressed, except that remarkably β-S lines can be observed on the free surface of the sample heated at 1200 °C. The typical powder XRD patterns are shown in Fig. 8 for glasses L4 and L8, heated at 900 and 1200°C for 1 h. Fig. 9 shows the relative X-ray intensity of the β-S peak to the β-Q peak, $I_{s,111}/(I_{s,111} + I_{Q,100})$, as a function of heating temperature for N, L0 and L4 glasses. The relative β-S content increased with increasing temperature, consistent with that usually observed in spodumene-containing glass–ceramics. Moreover, as $La_2O_3$

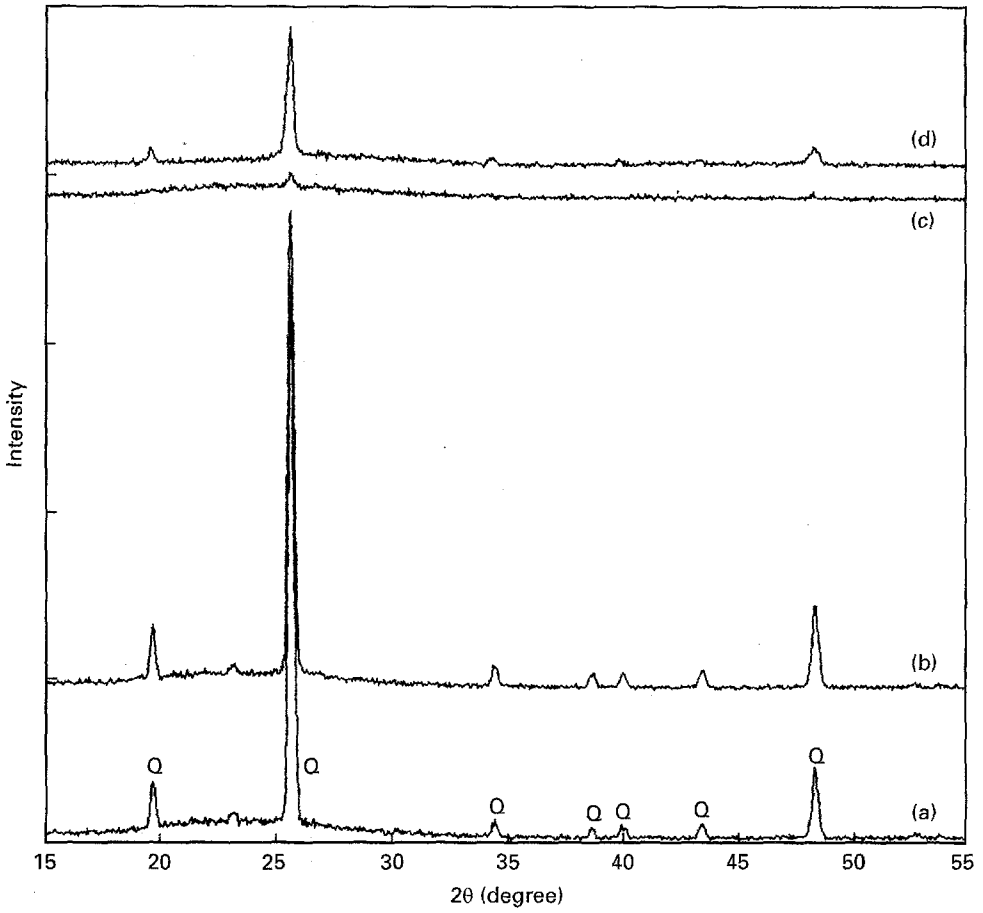


*Figure 7* Powder XRD patterns to examine the crystallization of glass to β-quartz ss for the (a) N, (b) L0, (c) L4, and (d) L8 glasses heated at 800 °C for 1 h (Q: β-quartz ss).

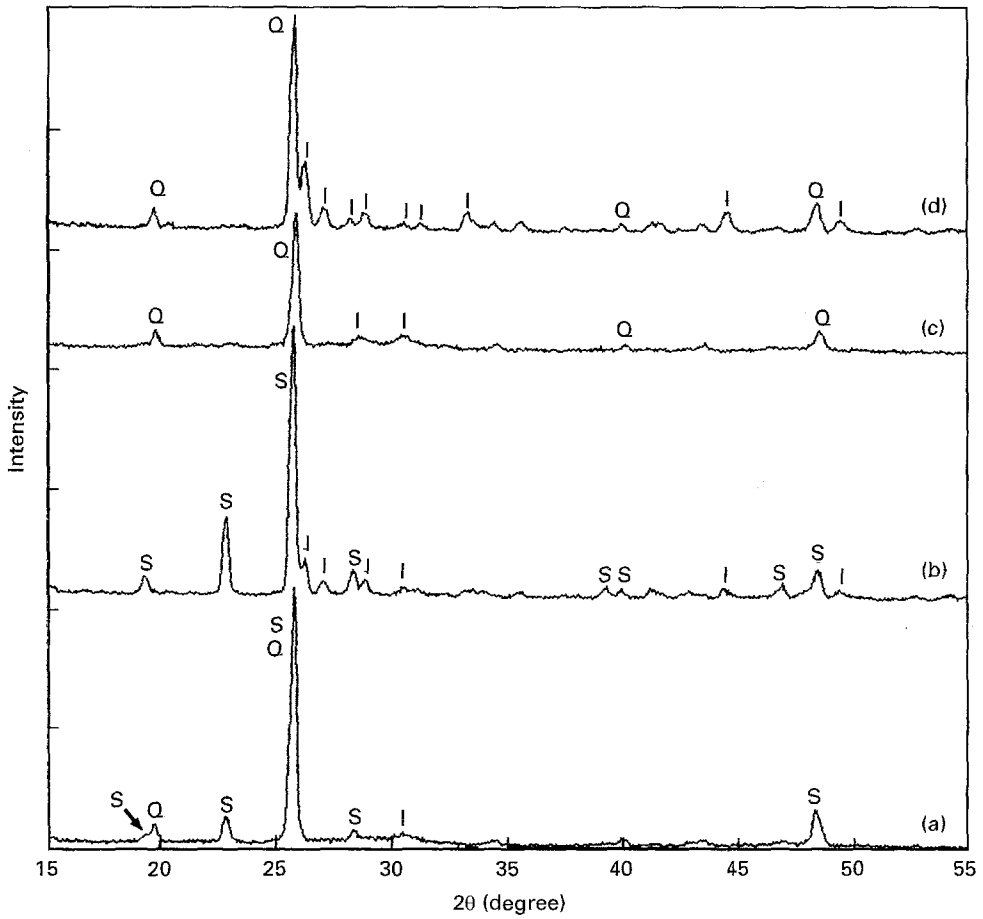


*Figure 8* Powder XRD patterns of the L4 samples heated for 1 h at (a) 900 °C and (b) 1200 °C and L8 samples heated for 1 h at (c) 900 °C and (d) 1200 °C. (Q: β-quartz ss, S: β-spodumene, I: La-containing compound).

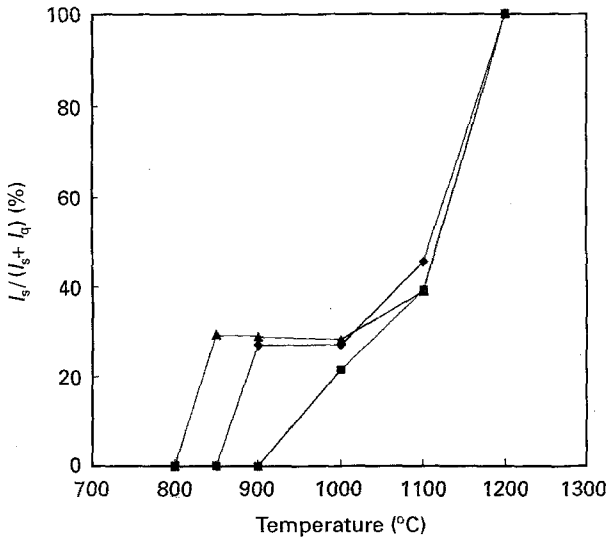


*Figure 9* The relative X-ray intensity of β-S to β-Q, $I_{s,111}/(I_{s,111} + I_{Q,100})$, as a function of heating temperature for the $La_2O_3$-doped samples. Key: ■ N; ◆ L0; ▲ L4.

increased, the onset temperature for Q → S transformation shifted to a lower temperature, while according to Fig. 7 the G → Q transformation was reduced. It is thus concluded that, as described in Section 3.2 for the $Y_2O_3$-doped glasses, the increase in Q → S kinetics in the $Y_2O_3$-doped glasses can be attributed to the decrease in the stability of the β-Q formed. It was also found that samples L0 showed no extra phase in addition to β-Q and β-S, while samples L4 and L8 heated at temperatures ≥ 900 °C exhibited an extra phase (see Fig. 8) which contained La, Al, and Si according to energy dispersive X-ray (EDX) analysis.

Fig. 10a–d show the typical microstructures for the L8 samples. Fig. 10a shows the microstructure of the sample nucleated at 700 °C for 10 h and then crystallized at 850 °C for 5 h. The large, ellipsoidal particles are $La_2O_3$, $Al_2O_3$, and $SiO_2$-containing phase, according to EDX analysis. The fine particles are β-quartz ss. According to Fig. 10b–d, as the sample was further heated at a higher temperature, the particles of both phases underwent a coarsening effect (Ostwald ripening).

## 3.4. Activation energy for crystal growth of the glass L8

Since glass L8 exhibited prominent bulk crystallization of β-Q phase, the activation energy for β-Q crystal growth was studied by DTA. The as-annealed glass

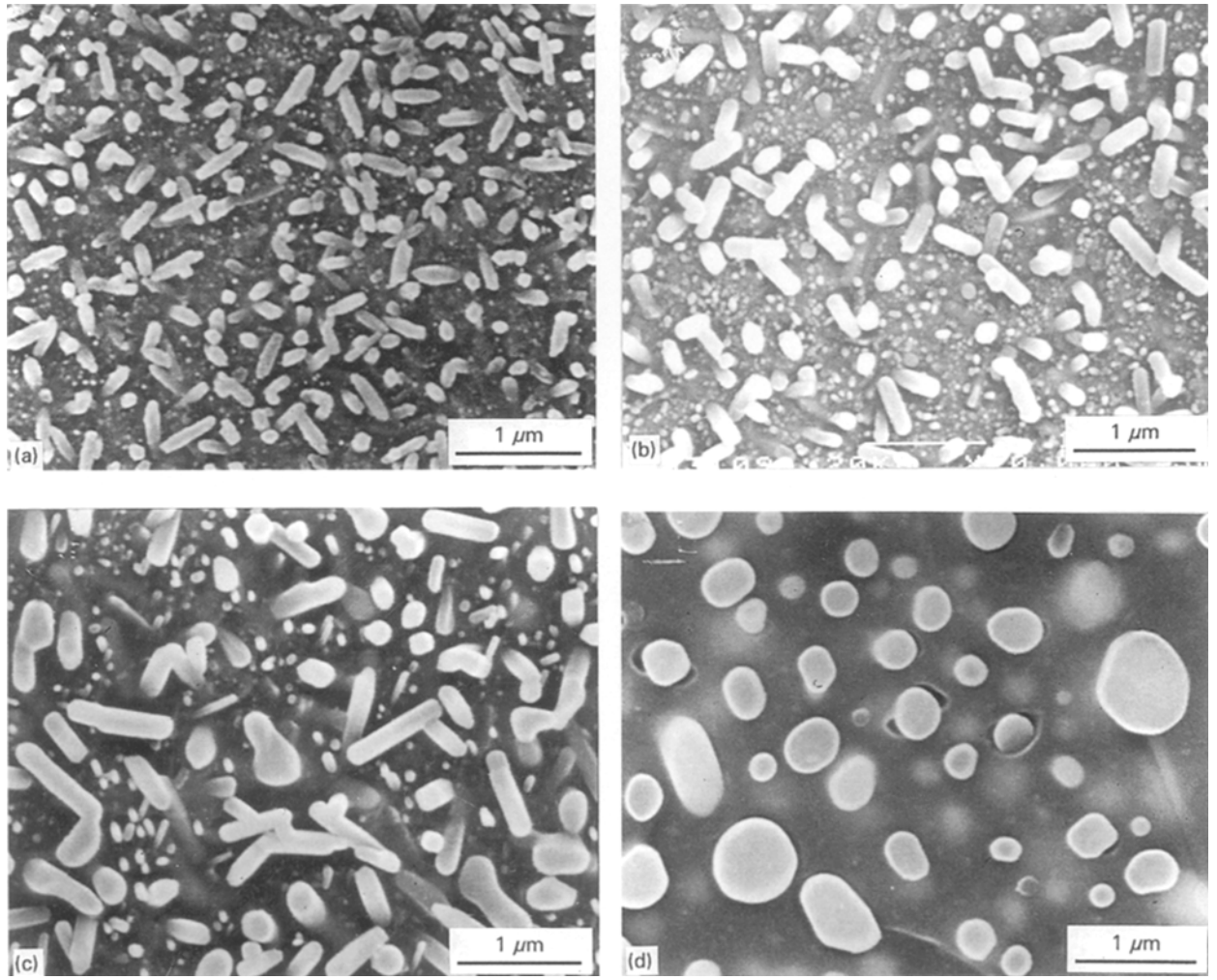


*Figure 10* SEM pictures showing the microstructures of the crystallized L8 samples. All samples were firstly nucleated at 700 °C for 10 h and crystallized at 850 °C for 5 h. Samples were then heated at (b) 1000 °C, (c) 1100 °C, and (d) 1200 °C for 10 h. (Bar = 1 μm).

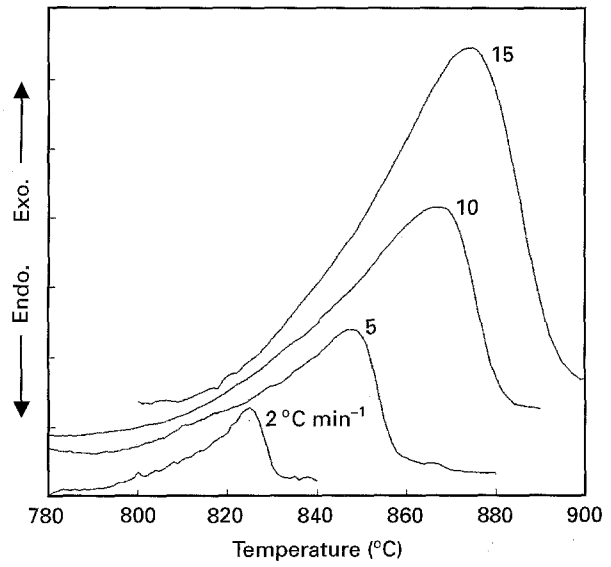


*Figure 11* DTA curves with various heating rates for the peak caused by the crystallization in glass L8.

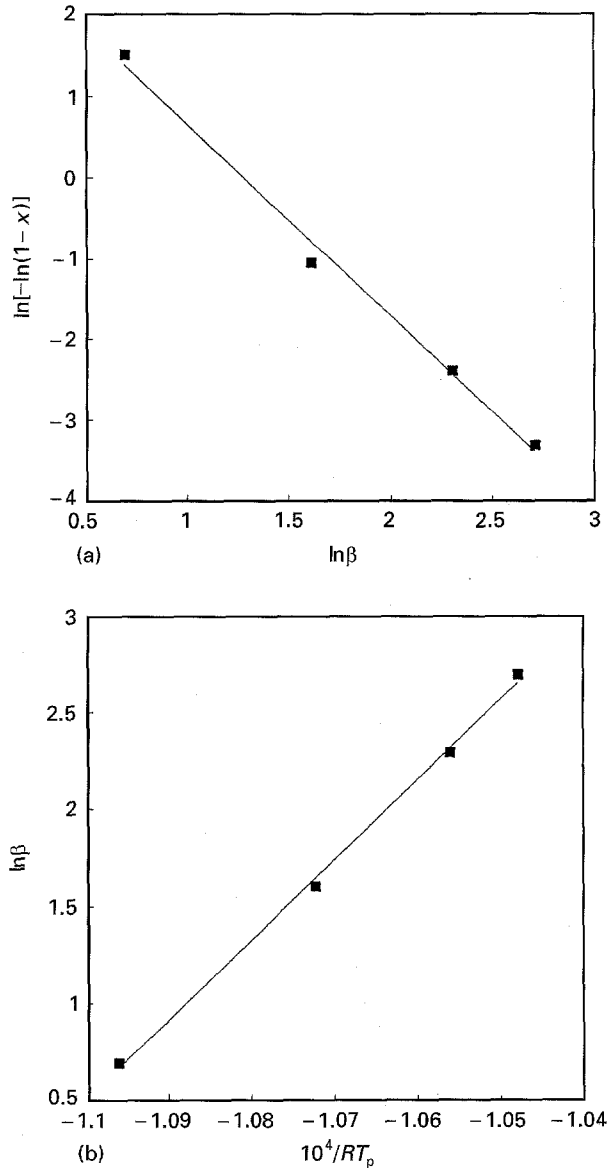


*Figure 12* Plot of (a) ln[-ln(1 − x)] versus lnβ and (b) lnβ versus $10^4/RT_p$ for the L8 glass.

was crushed into a powder (60–80 mesh). Samples were then heated at 700 °C for 10 h, during which the nuclei were formed, resulting in nearly saturated samples. Thus, crystal growth should have occurred on a fixed number of nuclei during the DTA run [7]. The DTA curves measured at different heating rates ($\beta = 2$–$15\ K\,min^{-1}$) are shown in Fig. 11. The peak position, $T_p$, shifted to higher temperatures as the heating rate increased. The activation energy for crystal growth, $E_c$, and the Avrami exponent, $n$, were determined according to the modified JMA equation [8]:

$$\ln[-\ln(1-x)] = -n\ln\beta - mE_c/RT + \text{constant} \quad (1)$$

where $x$ is the fraction crystallized, and $m$ and $n$ are integers, the values of which depend on the morphology of the growth. For a glass containing a sufficiently large number of nuclei, $m$ is equal to $n$ [7]. Therefore, according to Equation 1, the $n$-value can be calculated at any fixed temperature from the plot of ln[-ln(1 − x)] versus lnβ (see Fig. 12a), and is about 2.4. This value indicates that a crystal growth mechanism of two to three dimensions. Moreover, it has been shown that the volume fraction of crystal at $T = T_p$ is the same irrespective of β [7]. Thus, according to Equation 1 the $E_c$ value can be obtained from the slope of the plot lnβ versus $1/RT_p$ (see Fig. 12b) and is about $418\ kJ\,mol^{-1}$.

## 4. Conclusions

1. Adding ≥ 4 mol% of $YO_{3/2}$ or 8 mol% of $LaO_{3/2}$ effectively improved the control of the crystallization process of the glass. $Y_2O_3$ did not effectively induce bulk crystallization of β-quartz ss, but can reduce the rate of surface crystallization. $La_2O_3$ completely suppressed the surface crystallization and promoted a uniform, bulk crystallization of β-quartz ss.

2. For both the $Y_2O_3$- and $La_2O_3$-doped glasses, the kinetics for glass crystallization to β-quartz ss was delayed as the doping level increased. Except the 8 mol% $LaO_{3/2}$-doped glass in which no β-spodumene was formed, the kinetics for the β-quartz ss to β-spodumene transformation for the doped glasses was enhanced compared with that for the undoped glass.

3. For the 4 and 8% $YO_{3/2}$-doped compositions, the amount of β-spodumene relative to β-quartz ss revealed an anomalous decrease with temperature in a particular temperature range. This result can be explained by the surface crystallization characteristic, which induced an overlap of crystallization and the β-quartz ss to β-spodumene transformation.

4. Glass doped with 8 mol% of $LaO_{3/2}$ exhibited an Avrami exponent of about 2.4 and an activation energy for crystal growth of β-quartz ss of about $418\ kJ\,mol^{-1}$.

## Acknowledgements

This work was supported by the National Science Council of the Republic of China for financial support under Contract NSC83-0405-E036-003.

## References


1. H. SCHEIDLER and E. RODEK, *Amer. Ceram. Soc. Bull.* **68** (1989) 1926.
2. Z. STRNAD, "Glass-Ceramic Materials, Glass Science and Technology", Vol. 8 (Elsevier, Amsterdam, 1986) p. 85.
3. R.R. TUMMALA, *J. Amer. Ceram. Soc.* **74** (1991) 895.
4. J.U. KNICKERBOCKER, *Amer. Ceram. Soc. Bull.* **71** (1992) 1393.
5. A. KUMAR, P.W. McMILLAN and R.R. TUMMALA, US Patent 4301324, November (1981).
6. P.W. McMILLAN "Glass-Ceramics", 2nd Edn (Academic Press, London, 1979) p. 225.
7. X.J. XU, C.S. RAY and D.E. DAY, *J. Amer. Ceram. Soc.* **74** (1991) 909.
8. K. MATUSITA, T. KONATSU and R. YOROTA, *J. Mater. Sci.* **19** (1984) 291.



*Received 10 March*
*and accepted 7 November 1995*